Multifunctional Soft Gripper With Microneedles and Integrated Sensing for Robotic Fabric Handling

Subyeong Ku, *Member, IEEE*, Byung-Hyun Song, Taejun Park, Ho-Young Kim, and Yong-Lae Park, *Member, IEEE*

***Abstract*—This study proposes a multifunctional soft robotic gripper for handling fabrics that are unstructured and flexible. The multifunctional finger design allows the gripper to change its gripping mode between pinching and suction, depending on the air permeability of the fabric. The gripper is able to separate a single fabric from a stack with success rates of 95% and 100% for air-permeable and non-air-permeable fabrics using pinching and suction, respectively. The actuation time is as short as 0.65 s for the two gripping modes. During gripping, the compliant body structure distributes the stress and endures up to 50 N of pressing force at the tip, thus preventing damage to both the fabrics and the gripper. In addition, the integrated air pressure sensor detects the contact and enables control of the pressing force. Before gripping the fabric, the air permeability of the fabric is first detected by the pressure sensor in the vacuum regulator, and the gripping mode is then selected accordingly. The proposed gripper demonstrates reliability in performance and structural robustness over 10 000 cycles of repeated actuation, showing a high potential in automation of garment manufacturing, in which repetitive and delicate handling of various types of fabrics is one of the key requirements.**

***Index Terms*—End effectors, integrated design, manufacturing automation, soft robotics.**

Manuscript received 11 February 2023; revised 28 July 2023; accepted 31 October 2023. Date of publication 5 December 2023; date of current version 18 April 2024. Recommended by Senior Editor G. Berselli. This work was supported in part by SNU-Hojeon Garment Smart Factory Research Center funded by Hojeon Ltd. and in part by the National Research Foundation under Grant RS-2023-00208052, Grant NRF-2018-052541, and Grant NRF-2021R1A2C2093790. *(Corresponding author: Yong-Lae Park.)*

Subyeong Ku was with the Department of Mechanical Engineering, Seoul National University, Seoul 08826, South Korea. He is now with the Smart Manufacturing Technology R&D Center, Korea Automotive Technology Institute, Siheung 15014, South Korea (e-mail: sbku@katech.re.kr).

Byung-Hyun Song, Taejun Park, Ho-Young Kim, and Yong-Lae Park are with the Department of Mechanical Engineering, Institute of Advanced Machines and Design (IAMD), Institute of Engineering Research, Seoul National University, Seoul 08826, South Korea (e-mail: bh.song@snu.ac.kr; taejunpark@snu.ac.kr; hyk@snu.ac.kr; ylpark@snu.ac.kr).

This article has supplementary material provided by the authors and color versions of one or more figures available at https://doi.org/10.1109/TMECH.2023.3334246.

Digital Object Identifier 10.1109/TMECH.2023.3334246

I. Introduction

DEMANDS for automated fabric handling continue to grow in the garment manufacturing industries that are particularly labor-intensive. Despite recent advances in robotics and gripper technologies, automation in garment production is still highly limited due to the various characteristics of fabrics, such as air permeability, thickness, friction coefficient, and stiffness [1], [2], [3], [4], all of which make fabrics complex and unpredictable in terms of their behaviors. To address this issue, grippers made of soft materials with improved adaptability have been proposed as an alternative to conventional rigid grippers. The actuation mechanisms of the soft grippers include pneumatic [5], [6], [7], tendon-driven [8], [9], [10], vacuum jamming [11], and vacuum suction [12], [13], [14]. However, these grippers are specialized in only a few specific properties of fabrics and therefore do not provide versatility required to handle the wide range of different fabrics.

Soft materials have also been used to enhance the versatility of the conventional grippers. The soft spiral gripper was able to grasp objects with various shapes but was unable to hold fabric without crumpling it [15]. The self-sealing suction gripper was capable of dynamically changing the size of the suction cavity and grasping different shapes but was not suitable for handling porous fabrics [16]. The vacuum-actuated needle gripper was effective in picking up both porous and nonporous fabrics but had difficulties separating a single sheet of porous fabric from the stack due to the undesired vacuum force [17]. While each of these developments provide unique solutions depending on different fabric properties, they still show limitations in handling a wide range of fabrics used in the garment industries.

Therefore, we identified three key requirements for a versatile gripper to handle fabrics: single sheet separation from a stack [18], [19], [20], adaptable operation for fabrics with different air permeability [21], [22], and the ability to grip fabrics with different properties, such as friction, stiffness, rigidity, etc., without damaging the fabric [1], [2], [3], [4]. In addition, the gripper needs to be equipped with sensors for automated operations and precise control of the pressing force. This is particularly important since the capability of single sheet separation is highly dependent on the normal force applied to the fabric stack by the gripper. There also exists the minimum vertical pressing force to buckle the fabric, required for grasping by

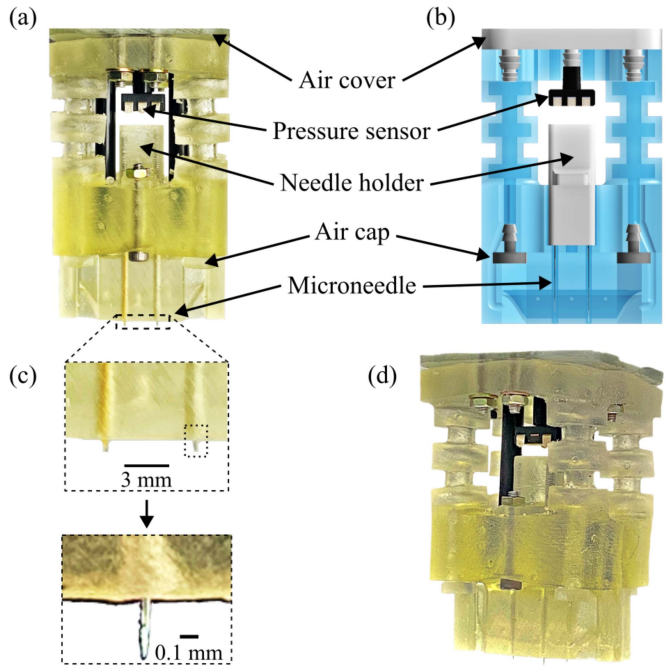

Fig. 1. (a) Photo and (b) schematic front view of the proposed gripper showing the main components. (c) Magnified views of the embedded microneedles. (d) 3D view of the gripper.

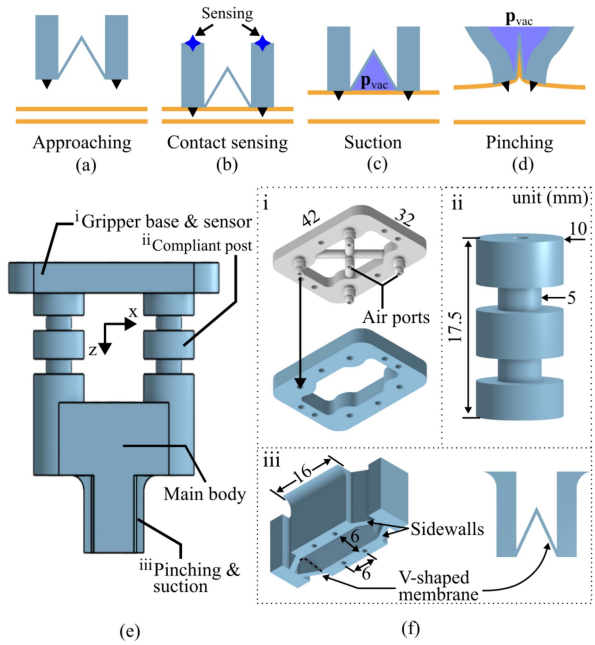

Fig. 2. (a)–(d) Gripper operation procedure corresponding to combined suction and pinching working principles. (e) Overall design and main components of the gripper. (f) Details of the components. i. Air cover and gripper base for integration of barometric pressure sensor. ii. Bellow-shaped compliant post. iii. Gripper fingers and a membrane for pinching and suction modes.

pinching. These forces are unique to each fabric type depending on its frictional coefficient and flexural rigidity [23], [24], [25]. The gripper also needs to be easy to fabricate and maintain. Therefore, we propose a multifunctional soft robotic gripper that satisfies these requirements and overcomes the limitations of the aforementioned grippers.

Common operating principles used by fabric handling grippers involve pinching, intrusion, adhesion, electrostatic, and pneumatic actuation, each with its own advantages [26], but there is no general method to handle soft and flexible fabrics. We combined two different principles, suction and microneedle-assisted pinching [see Fig. 1(a)–(c)], in a single structure to target both types of fabrics with and without air permeability. To develop a structure capable of both pinching and suction, we applied soft robotics technologies with a high degree of freedom. We also adopted a compliant structure by employing bellow-shaped posts and soft materials, which allowed gripping of the target object (e.g., fabric) even with nonideal contacts and provided tolerance to an excessive load during gripping. Also, an air chamber was made by sealing the bellow-shaped structure and used to measure the internal pressure during the contact with the fabric.

With recent 3D printing technologies, it is now possible to directly print and assemble soft grippers and their parts that had to be fabricated using multiple molds previously [27], [28], [29], [30]. Instead of going through manual fabrication steps involving molding and casting, susceptible to human errors, we utilized 3D printing techniques to fabricate parts with uniform quality, consistent performance, and high structural complexity that permits multifunctionality of the grippers [see Fig. 1(d)].

Since the required range of pressing force varies from fabric to fabric, a sensor was integrated into the gripper to measure and control the pressing force. By employing a commercial air pressure sensor that measures the changes in the internal pressure of the proposed gripper, we were able to estimate and control the pressing force while maintaining a compact form factor of the gripper. This is particularly important since the contact area on the fabric allowed for quality control in the garment production process can be as small as 6.34 mm from the edge [31], thus a bulky system for actuation and sensing is not suitable which was hard to achieve with conventional methods.

Thereby, the proposed gripper demonstrates reliability, robustness, and flexible operation adaptable to varying fabric properties, as well as potential for safe collaboration with human operators.

II. Design

A. Operation Procedure

Grasping first starts with approaching the target fabric and sensing the contact [see Fig. 2(a) and (b)]. For the suction mode, a vacuum pressure is applied between the membrane and the fabric [see Fig. 2(c)]. For the pinching mode, a vacuum pressure is applied inside the membrane to deform the fingers for pinching [see Fig. 2(d)].

B. Integrated Pressure Sensor and Compliant Structure

The proposed gripper has four main features in design: multifunctional actuation of pinching and suction, easy assembly and

replacement of microneedles, structural compliance for stable gripping, and an integrated pressure sensor. The dimensions of the gripper were selected based on the length of a commercial microneedle, 35 mm (HL-001 Series, HLMedical). The overall shape and the components of the gripper are shown in Fig. 2(e). The total height of the gripper including its cover is 53 mm with a width of 42 mm. With this configuration and the compliant structure, the gripper was able to adjust the tip position horizontally up to ± 3.7 mm on the xy-plane.

The top half of the gripper [see Fig. 2(e)] was designed to provide compliance and contact sensing ability. A pneumatic pressure sensor was connected to a 3D-printed air cover that was used as a mechanical connector to a robot manipulator [see Fig. 2(f)-i]. Pressure sensing is made possible by four compliant posts that deform to create a change in internal pressure. The air cover has five barbed air ports, each connected to the compliant post and a barometric pressure sensor. The air chambers of the compliant posts are connected through pipes, and their total pressure is measured by the barometric pressure sensor in the center. The inner diameter of the pipe and the port was selected to be 1.4 mm, the smallest hole that can be made by 3D printing without clogging to minimize the passive volume.

The four bellow-shaped posts placed at four corners of the gripper also provide structural compliance, minimizing undesired deformations of the fingertip during contacts with fabrics [see Fig. 2(f)-ii]. Each post bends according to the orientation and contact force, stabilizing the position of the fingertips normal to the fabric. More detail will be discussed in Section III.

C. Soft Multifunctional Gripper

The bottom half of the gripper in Fig. 2(e) was designed to perform two independent actuation modes. During the contact with fabric, a cavity is formed, enclosed by the V-shaped membrane, the fingertips, and the fabric [see Fig. 2(c)]. The vacuum pressure applied in this space activates the suction mode to grasp non-air-permeable fabrics. If the target fabric is air permeable, the vacuum pressure is applied in a separate space between the membrane and the gripper [see Fig. 2(d)], pulling the membrane upward and closing the fingertips, consequently enabling the pinching motion. Since the entire structure is printed as a whole, the pinching fingers and the sidewalls have the same material properties. However, since the fingers must be flexible enough to be easily bent by the vacuum force without buckling or collapsing, the sidewalls were oriented at an angle, guiding the fingers to bend to the center [see Fig. 2(f)-iii].

D. Analysis

The force applied to the fabric by the gripper differs based on the actuation modes. This relationships are expressed as

$$F_{\text{suction}} = A_{\text{eff}} \cdot p_{\text{vac}} \tag{1}$$

$$F_{\text{pinching}} = 2F_f = 2\mu F_n = 2\mu A_f \cdot (p_{\text{vac}} - p_0) \tag{2}$$

where F_{suction} and F_{pinching} are the suction and the pinching forces of the gripper, respectively, A_{eff} is the effective suction area under vacuum, p_{vac} is the vacuum pressure applied between the fabric and the membrane, F_f is the friction force, μ is the friction coefficient between the gripper and the fabric, F_n is the normal force created by the pinching motion, and A_f is the pinching area, p_0 is the minimum pressure when the contact occurs, which is unique to each fabric [see Fig. 3(a) and (b)].

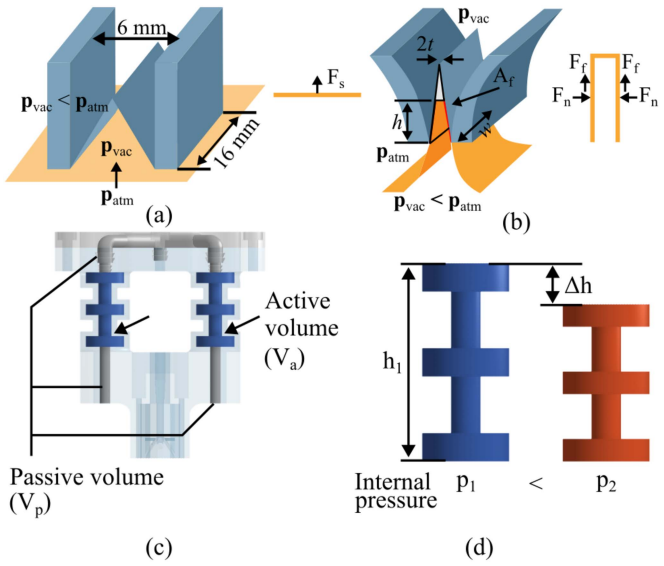

Fig. 3. (a) Suction mode and free body diagram. (b) Pinching mode and free body diagram. (c) Closed pneumatic system schematic composed of passive and active volumes. (d) Initial state (Left) and compressed state (Right).

In both actuation modes, the exerted force is affected by the contact area (1) and (2). For the suction mode, we assumed that the actual contact area under vacuum is smaller than the designed dimensions due to the compliance of the vacuum pad [32]. The effective area A_{eff}, found experimentally, is 40 mm^2, smaller than the contact area (126 mm^2) in the design. In the pinching mode, it was assumed that the gripper holds the fabric sheet by closing the fingers to the center without slipping from the fabric. The contact area between the gripper and the fabric A_f, affected by the thickness of the fabric, was determined through simulation.

To separate a single sheet of fabric from a stack, the gripper must press the fabric with an appropriate force, which will be discussed in detail in Section III. Therefore, a sensor is required to measure the pressing force to operate the gripper properly. The gripper experiences changes in the internal volume as the compliant posts are deformed during pressing. According to Boyle's law, the pressure increases as the volume decreases in a closed system. We assumed that the closed system in the gripper is composed of the active volume (V_a), which changes when the external force is applied, and the passive volumes (V_p) that remains consistent [see Fig. 3(c)]. V_p is 213.91 mm^3 in the design, independent of the external force.

Using the design parameters in Fig. 3(d), the relationships between the initial and the final pressures and the volume are expressed as

$$p_1 \cdot V_1 = p_1 \cdot (V_p + V_a) = p_2 \cdot V_2 \tag{3}$$

$$V_2 = 4A_{eq} \times (h_1 + \Delta h) + V_p \tag{4}$$

where p_1 is the initial internal pressure with the external force of zero and is equivalent to the ambient pressure of 100.6 kPa, p_2 is the final internal pressure when external force is applied, V_1 and V_2 are the corresponding volumes, A_{eq} is the equivalent cross sectional area of the bellow-shaped post approximated to a cylinder (5.31 mm^2), h_1 is the initial height of the bellow-shaped post (18.7 mm), and Δh is the height change due to the pressing force. These equations can be rearranged to express p_2 as

$$p_2 = \frac{p_1 \cdot (V_p + V_a)}{4A_{eq} \times (h_1 + \Delta h) + V_p}. \tag{5}$$

Given the pressure p_2, the change in height Δh can be calculated, and by finding the relationship between the Δh and the pressing force, the contact force can be obtained from the measurements of p_2. We employed a pneumatic pressure sensor (XGZP6847-040KPGPN, CFSensor) that measured the internal pressure of the bellow-shaped compliant posts and determined the relationship between the pressing force and Δh through a tensile test.

E. Simulation

COMSOL Multiphysics® (COMSOL) was used to conduct finite element analysis (FEA) to optimize the gripper design features and identify design parameters. The material used to make the gripper was a soft photopolymer resin for stereolithography (SLA) 3D printing (Elastic 50 A, Formlabs). To determine the design parameters, we performed a tensile test using a motorized test stand (Mark-10, Mark-10 Corporation) for a specimen of the printed elastomer to obtain a Neohookian parameter of the material [see Fig. 4(a)]. The Neohookian model is suitable for small strains [33], and the test result is shown in Fig. 4(b).

The pinching force is determined by the fabric's coefficient of friction and the normal force (2). Since the normal force is characteristic of the gripper tip structure, we optimized the fingertip design to maximize the normal force, as summarized in Fig. 4(c) and (d). First, we compared the normal force between variations of the side walls (flat and curved) and the membrane (flat and V-shaped). The normal force was higher with flat sidewalls (Shape 2) than with curved ones (Shape 1). This is because the two flat walls positioned at an angle are easier to fold than the curved walls. In the same manner, the V-shaped concave membrane (Shape 3) was able to generate a higher normal force than the flat one (Shape 2) and employed in our final design.

Next, we identified three design variables by simulation, which affected the volume of the suction cavity and normal force based on the Shape 3 [see Fig. 4(e)]. The suction cavity indicates the space between the contact surface and the membrane in which vacuum pressure is applied, and its volume is determined by the angle of the V-shaped membrane (θ) and the offset (d_{offset}). Since pinching occurs by folding the membrane, we assumed that the thickness of the membrane (t_{membrane}) would affect the normal force. Therefore, we simulated the normal force in response to the input pressure for different d_{offset} and t_{membrane} for a fixed θ of 35°. The result in Fig. 4(f) shows that the normal force increases as t_{membrane} and d_{offset} decreased. Then, with the

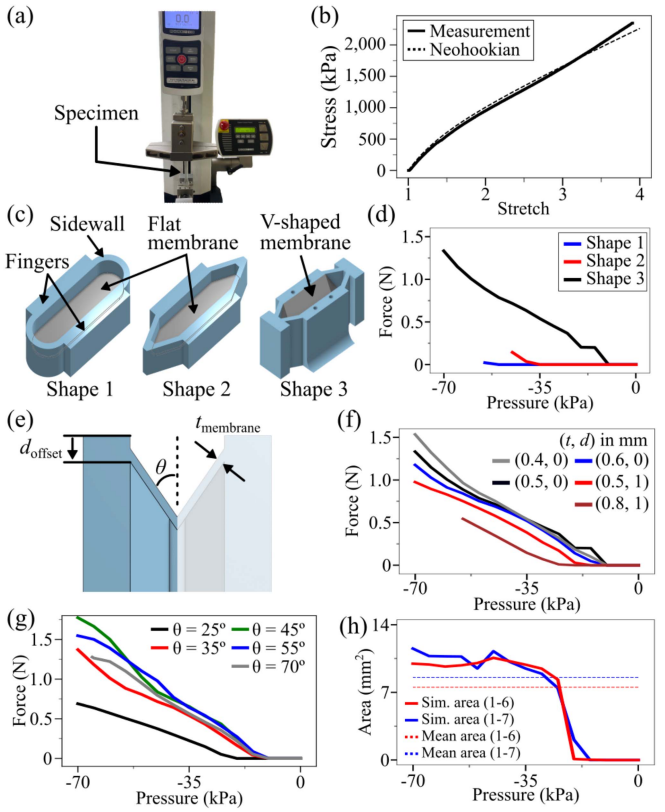

Fig. 4. Simulation results of normal force in pinching. Tensile test setup (a) and result (b). (c) Membrane shapes for simulation. (d) Normal force in response to input pressure for different membrane shapes. (e) Optimization parameters of the V-shaped membrane. (f) Normal force in response to input pressure for different thicknesses and offsets of the V-shaped membrane. (g) Normal force in response to input pressure for different angles θ. (h) Contact area change in response to input pressure for two types of fabrics: thick and air-permeable fabric (1–6, red) and thin and air-permeable fabric (1–7, blue). Refer to Table 1 for the fabric.

thickness and the offset of 0.5 mm and 0 mm, respectively, we conducted simulation to predict the normal force with varied θ from 25° to 70° [see Fig. 4(g)]. The normal force showed the maximum value at an angle of 45°, significantly decreasing as the angle became smaller. While higher normal forces can be obtained with t_{membrane} of 0.4 mm or less, we chose a thickness of 0.5 mm for stable 3D printing and higher yield. Also, the angle θ was chosen to be 35° to make a balance between the normal force and the suction cavity volume.

As described in Section II-D and (2), pinching force is proportional to contact area, A_f, which differs depending on the target fabrics, and was determined through simulation. We simplified the simulations, varying only the thickness parameter and set the properties of all simulated fabric as rubber (Young's modulus 100 MPa). Simulations were conducted for all air-permeable fabrics, and we have visualized results for fabrics 1–6 and 1–7 of Table I in Fig. 4(h). These fabrics were selected to show the effect of thickness on the contact area, as they have very similar coefficients of friction but a large difference in thickness. The average contact areas were calculated to be 7.53 mm^2 and 8.54 mm^2 for the 1–6 and the 1–7 fabrics, respectively. The

TABLE I
INFORMATION ON THE FABRICS USED IN EXPERIMENTS

Fabric label	1–1	1–2	1–3
Composition	Polyester, Spandex	Recycled polyester	Polyester, Spandex
Permeability [mm/s]	32.8	255	872
Flexural rigidity [10^{-4} Nm]	3.89	6.41	13.2
Thickness [mm]	0.25	0.32	0.58
Coefficient of friction 1	2.48	3.73	2.14

1–4	1–5	1–6	1–7	2–1	2–2	2–3
Cotton, Hemp	Polyester, Spandex	Polyester, Spandex	Nylon	Nylon	PU-coated nylon	Polyester
628	56.9	15.3	49.8	0	0	0
6.13	3.88	13.6	2.96	3.91	6.34	12.0
0.31	0.23	0.35	0.15	0.07	0.2	0.46
3.27	2.36	1.15	1.33	1.37	1.73	1.54

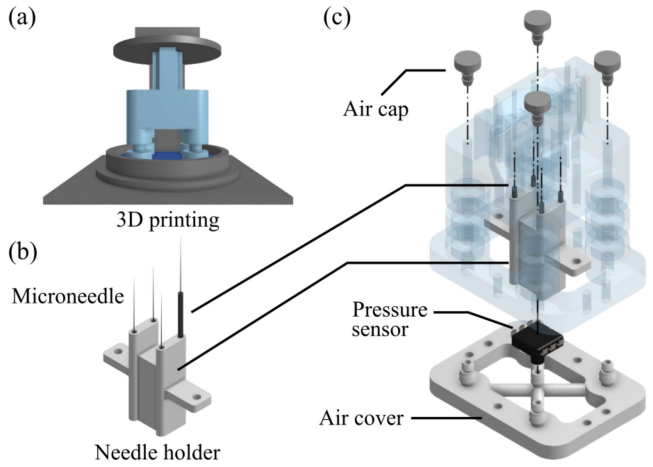

Fig. 5. Fabrication process. (a) 3D printing of the gripper body. (b) Microneedles and its holder. (c) Final assembly.

overall results show that the average contact area decreases as the fabric gets thicker.

F. Fabrication

The proposed gripper was fabricated using an SLA 3D printer (Form3, Formlabs) as a whole with soft photopolymer resin (Elastic 50 A, Formlabs) [see Fig. 5(a)]. After a simple postprocess of washing with isopropyl alcohol and UV curing (Form Cure, Formlabs), the gripper can be operated.

The air cover and the needle holder were also fabricated by 3D printing. The needle holder was designed to allow easy integration and replacement of off-the-shelf microneedles rather than direct embedment in the elastomer [see Fig. 5(b)], not requiring any additional alteration and facilitating easy replacement when damaged. The final assembly of the proposed gripper is described in Fig. 5(c).

III. EXPERIMENTS

We first conducted experiments to check the feasibility of the two actuation modes in a single gripper structure. We then tested the pinching and the suction performances. The experiments were conducted with seven types of air-permeable fabric and three types of coated fabric with no air permeability.

The gripper was mounted at the end of an industrial robot arm (UR5e, Universal Robots), and the holding force was measured using a precision scale (Pioneer PAG4102, OHAUS). A test fabric (60×70 mm^2) was placed on the scale with one edge fixed and was lifted by the gripper and the maximum pinching force was measured. To determine the maximum lifting force by suction, mass was increasingly added to a stainless-steel container and was lifted using the suction mode of the gripper. We also conducted experiments to measure the air permeability and the flexural rigidity of the ten fabrics, the basic properties that affect the capability of suction and pinching, respectively. We used an air permeability tester (FX 3300-IV, TEXTEST) to measure the air flow rate based on ISO 9237. The flexural rigidity was also determined based on ASTM D1388 [34]. The measured properties of each fabric are summarized in Table I.

A. Multimodes Actuation in Single Structure

Upon contacting the target fabric, the proposed gripper performs either a pinch or a suction grip depending on the air permeability of the fabric. During the pinching mode, the two fingers of the gripper buckle the fabric sheet with friction for lifting up. If the gripper opens the fingers for releasing, the folded part of the fabric straightens out, and the fabric is naturally disengaged from the needles [see Fig. 6(a)].

To verify the damage-free operation of the gripper, the fabric samples were examined using a microscope after each actuation. No noticeable damages, such as penetration holes by the needles or folded lines from buckling, were observed [see Fig. 6(b)-left and 6(b)-right].

We placed an air-permeable fabric (1–1) on top of a non-air-permeable fabric (2–2) and attempted to grasp and separate a single sheet of fabric by both suction and pinching [see Fig. 6(c)-top]. The gripper succeeded in separating and picking up the air-permeable fabric with pinching. However, the gripper was not able to separate a single sheet from the stack, which is due to the suction force not effectively applied to the top air-permeable fabric sheet but applied to the bottom non-air permeable sheet. The same results were observed with other air-permeable fabrics (1–2 to 1–7). Next, the non-air-permeable fabric was placed on top [see Fig. 6(c)-bottom]. In this case, single sheet separation was successful with suction but not successful with pinching. The coated surface of the non-air-permeable fabric was inadequate for creating enough shear force and caused the fingertips to slip. Pinching was ineffective for all other non-air permeable fabrics (2–2 and 2–3).

Through this experiment, we verified that different gripping mechanisms were required depending on the air-permeability of the fabric. The different actuation modes were integrated in a single gripper structure.

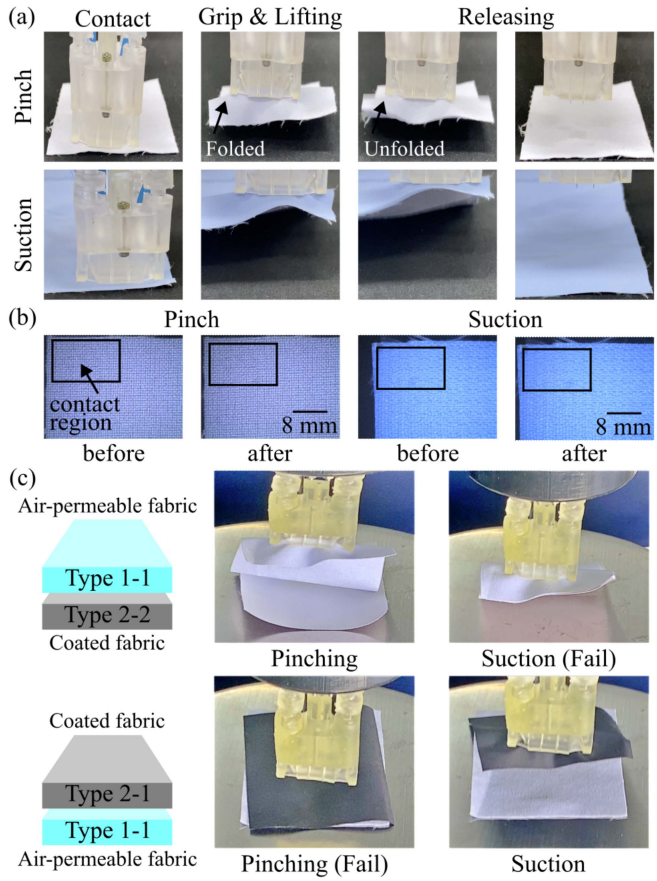

Fig. 6. (a) Operation sequence of the two actuation modes. (b) Comparison of the fabric surfaces before and after gripping showing no noticeable damages for both modes. (c) Results of multimodes actuation tests with air-permeable and nonair-permeable fabric types.

B. Pressure Response

The time required to reach the minimum vacuum pressure was recorded for each actuation mode, and the results are shown in Fig. 7(a)-top and 7(a)-bottom. It took 0.67 s. for suction and 0.65 s. for pinching to reach the minimum vacuum pressure of −80 kPa, and it took 0.43 s. and 0.44 s. for suction and pinching, respectively, to reach −72 kPa, 90% of the minimum pressure.

We analyzed the hysteresis of the pinching mode, as we used compressible fluid for actuation viscoelastic material for the gripper body. We placed red markers in the middle of both fingers of the gripper and traced their displacements over time using a motion analysis software package (ProAnalyst, Xcitex). Hysteresis was observed during the operation [see Fig. 7(b)], which however did not degrade the performance of the gripper since only the ON–OFF control of the minimum vacuum (zero) pressure was used for the actuation.

To measure the maximum suction force, the gripper lifted an object with suction for different pressure inputs (−30 kPa to −80 kPa). We increased the weight of the object until the gripper failed to lift it. Throughout the experiment, the gripper followed a procedure of approaching, pressing, and grasping the object by either actuation mode, and then lifted the object. The relationship between the suction force and the input pressure is shown in Fig. 7(c). The effective area for each pressure was calculated using the pressure and the mass values, and the force prediction model was derived using the average area of 40 mm^2, illustrated as a dotted line in Fig. 7(c). The gripper showed the maximum suction force of 3.1 N with the vacuum pressure of −75 kPa, which decreased linearly with the decrease of vacuum pressure.

The average pinching forces with the error bars for different input pressures for the 1–6 and 1–7 fabrics can be found in Fig. 7(d) and (e), respectively. The force was calculated by the model from the contact area, the fabric friction coefficients (see Table I), and the initial pressure at contact (p_0). We calculated the force using two initial pressure values obtained from the simulation and the experiment, which are illustrated as the blue and black solid lines, respectively. The p_0 values obtained from the experiments of seven types of air-permeable fabrics were between −40 kPa and −35 kPa (between −20 kPa and −15 kPa in simulation). It can be observed that the force calculated with the experimental value of p_0 shows a high correspondence to the measured values. Both the simulation and the actual measurement results suggest that the pinching force is proportional to the pressure difference. However, the two results showed a noticeable discrepancy since the simulation did not reflect the external force acting between the fabric and the floor [see Fig. 7(f)]. The friction force increased as the gripper pressed the fabric down, which interfered with the pinching motion. Therefore, pinching occurred at a lower p_0 in the actual experiment than in the simulation. Fig. 7(g) shows the maximum holding forces of the seven air-permeable fabric types, obtained from 10 trials using a vacuum pressure of −80 kPa. Overall, the experimental values showed a high correspondence with the theoretical values except for the 1–3 fabric. This is because the thickness of the 1–3 fabric is 0.58 mm that is larger than the protruding length of the microneedle (0.25 mm), so the needles were not able to fully penetrate the fabric. In this case, the microneedles were unable to effectively engage the fabric, resulting in the lower pinching force. The role of the microneedle was more closely investigated in an additional experiment.

To verify the repeatability of the gripper, we conducted cyclic tests with 10 000 cycles of applying and releasing the vacuum pressures in both the suction and the pinching modes [see Fig. 7(h)]. The subset in each plot shows the pressure change of the 5000th cycle. In both modes, the minimum pressures were consistent, confirming the performance and the structural robustness of the gripper finger and the membrane. Additional experiments showed that there were no damages at the tip of the needle, such as bending or wear, observed even after 5000 cycles of actuation [see Fig. 7(i)].

We also investigated the effect of the microneedles on the pinching force with the 1–7 fabric [see Fig. 8(a)–(c)]. Three conditions were tested: no microneedles, completely embedded needles, and needles protruded 0.25 mm. In all cases, the tip was pressed with a force of 2.5 N, and a vacuum pressure of −80 kPa was applied. The average holding forces were measured to be 0.53 N, 0.64 N, and 0.97 N for the three cases,

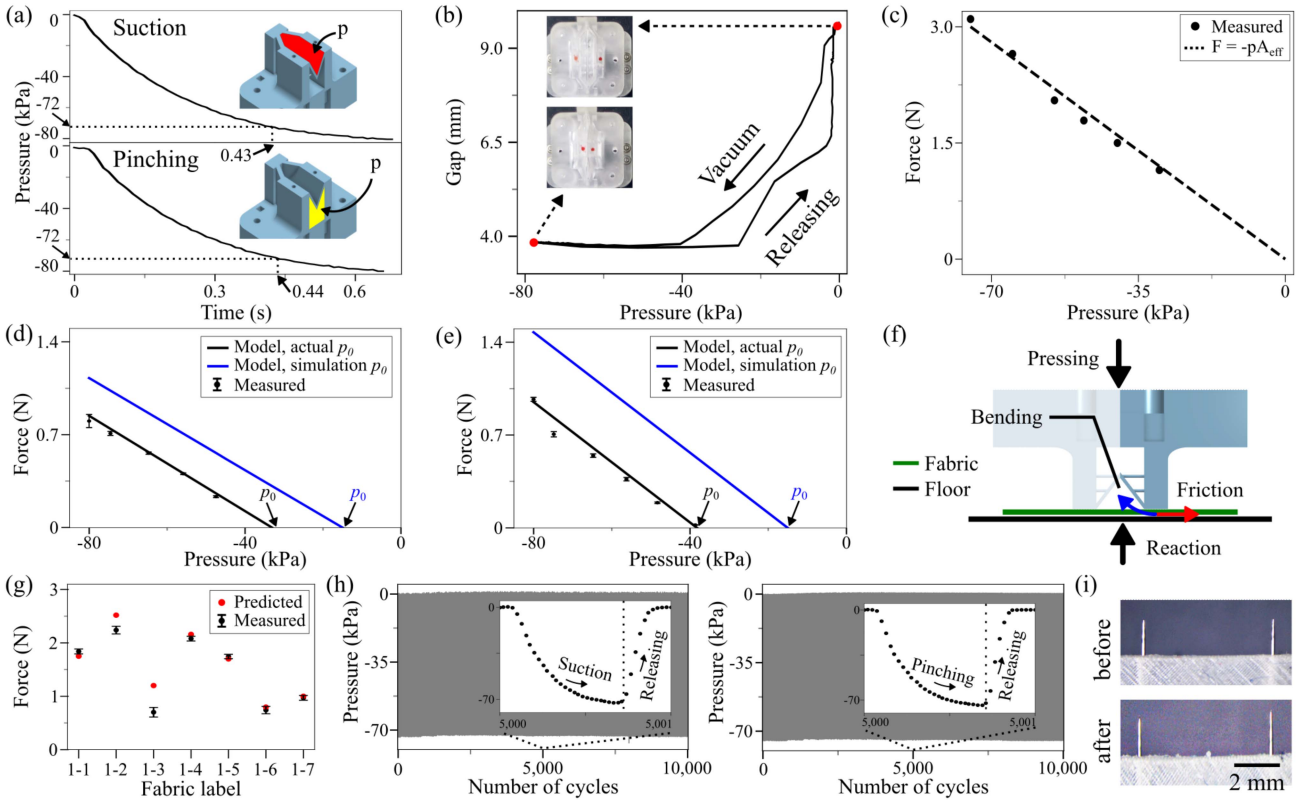

Fig. 7. Experimental results. (a) Pressure responses of suction and pinching. (b) Hysteresis during pinching. (c) Holding force measurements in comparison with model prediction for suction. (d) Pinching force measurements in comparison with model prediction for pinching of 1–6 and (e) 1–7 fabrics. (f) External forces during pinching. Friction (Red) hinders bending motion (Blue) of fingertips. (g) Maximum holding force of each air-permeable fabrics. (h) Repeatability test results of suction (Left) and pinching (Right). (i) Microscopic images of the embedded microneedles before and after 5000 actuation cycles.

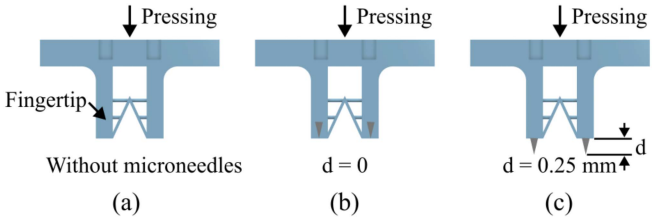

Fig. 8. Simplified schematics of the gripper tip and microneedles. (a) Without microneedles. (b) With microneedles with no protrusion and (c) 0.25 mm protrusion.

respectively. This demonstrates that the microneedles generate a larger holding force, which was further increased with protrusion of the needles.

C. Single-Sheet Separation

The force with which the gripper presses the fabric prior to gripping is an important factor that determines the success of gripping. As the appropriate force range for single sheet separation is unique to each type of the fabric, an experiment was conducted to identify the force range for the air-permeable fabrics [see Fig. 9(a)]. For all fabrics tested, single sheet separation was possible within the range of 0–3 N. For the 1–1 fabric,

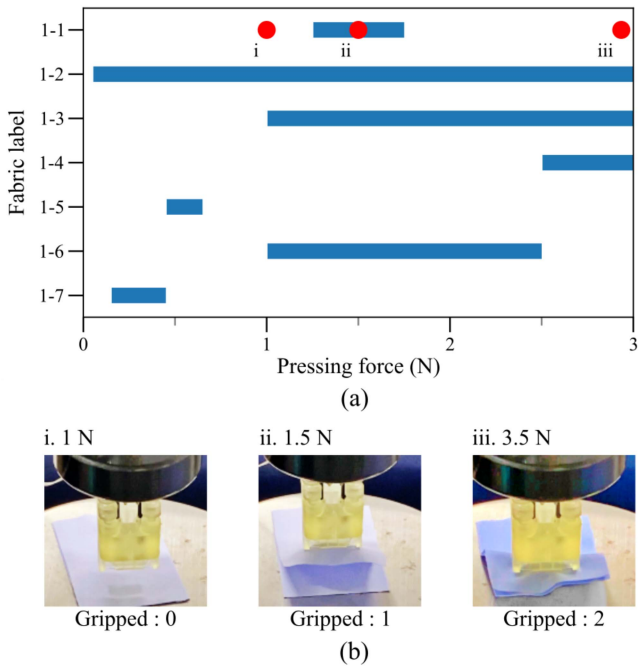

Fig. 9. (a) Force range to separate single sheet of air-permeable fabric. (b) Gripping results with pressing force of i. 1 N, ii. 1.5 N, and iii. 3.5 N.

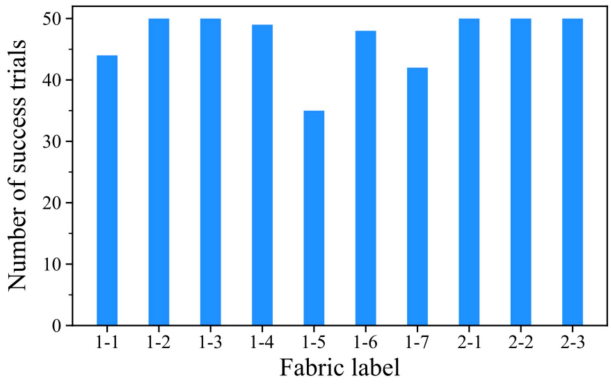

Fig. 10. Single sheet separation result. Pinching and suction modes were used for Type 1 and Type 2 fabrics. Each represents the number of successes out of 50 trials.

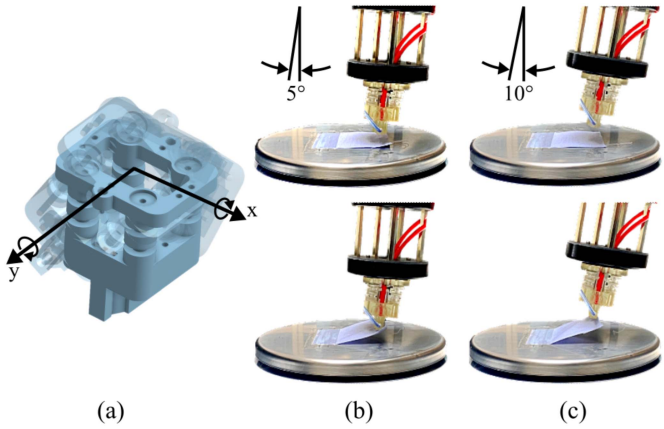

Fig. 11. (a) Contact experiment with angles. (b) Picking up fabric at angles of 5° and (c) 10° from the vertical axis.

a pinching experiment was conducted with different pressing forces [see Fig. 9(b)-i through 9(b)-iii]. The fabric cannot be picked up with pressing force less than the suggested range, and multiple sheets of fabrics are lifted if the force exceeds the range.

Using these findings of the specific pressing force ranges, the success rate of single-sheet separation for all fabric types and the appropriate actuation modes were recorded and depicted in Fig. 10. With suction, single-sheet separation was successful in all 50 trials without failures. However, pinching of air-permeable fabrics showed success rates ranging from 70% to 100%. Two main causes of the failures are the penetration of the microneedles through multiple fabric sheets and entanglement of the lint on the side of the fabric. Since the second case depends largely on the quality of the fabric rather than the performance of the gripper, only the first case was regarded as a functional failure. Other factors that affected the success rate were the thickness of the fabric and the range of the pressing force. The thicker the fabric and the larger the pressing force range, the higher the success rate was. The 1–5 and 1–7 fabrics, which showed lowest success rates, showed failures of 15 and 8 times out of the 50 trials, respectively. It must be noted, however, 12 out of the 15 failures for the 1–5 fabric and 6 out of the 8 failures for the 1–7 fabrics were actually functional failures. The other fabrics showed higher success rates, reaching the average of 93%.

D. Compliant Structure

As shown in Fig. 11(a), we experimented the compliance of the gripper by varying the approaching angle of the gripper to the fabric from -15° to $+15^\circ$ about the x- and y-axes with increments of 2.5°. The gripper successfully gripped and lifted the fabric with an attack angle of up to $\pm 10^\circ$ [see Fig. 11(b) and (c)] but failed when the attack angle exceeded these limits. Thus, the maximum allowable angles for the adjustment of inclination are $\pm 10^\circ$. This proves that the integrated compliant structure of the gripper provides a stable contact with existence of a load, and gripping is possible even if the contact is not perfectly perpendicular to the surface of the fabric. When the same experiment was conducted using the gripper without the compliant structure, pinching was successful only within the range of $\pm 2^\circ$.

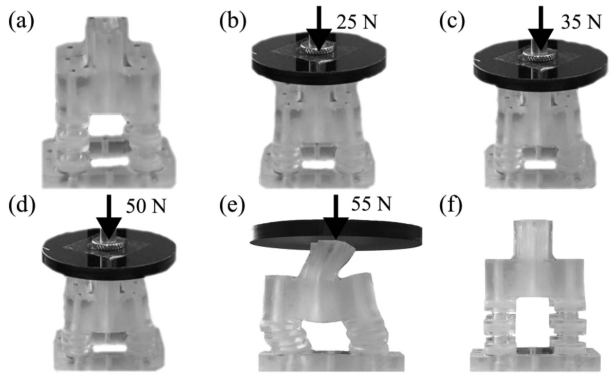

Fig. 12. Proposed soft gripper (a) before being pressed, with pressing forces of (b) 25 N and (c) 35 N, and (d) 50 N. (e) Pressing force of 55 N and (f) released from the pressing.

In addition, the compliance of the gripper body prevents fingertips from being damaged or deformed even under excessive load on the gripper. Since the gripper normally works in the range of the pressing force below 3 N, a force greater than this was considered as an excessive load. We observed the deformation in the fingertip of the gripper while applying force up to 50 N (16 times the normal pressing force), as shown in Fig. 12(a) through 12(d). Due to the compliant structure, no noticeable bending or tearing was observed, and the gripper tip was able to maintain a stable vertical contact with the surface of the target. Further investigation was conducted to determine the functional limit of the compliant structure. The gripper was subject to increasing vertical loads using a tensile tester (Mark-10) and a flat indenter, imitating the pressing force. When the pressing force of larger than 55 N was applied, the fingers of the gripper were significantly deformed [see Fig. 12(e)], making the gripper not functional properly for pinching. However, after unloading, the gripper restored to its original shape without any permanent damages in the compliant structure and the fingers [see Fig. 12(f)]. Therefore, the functional limit of the pressing

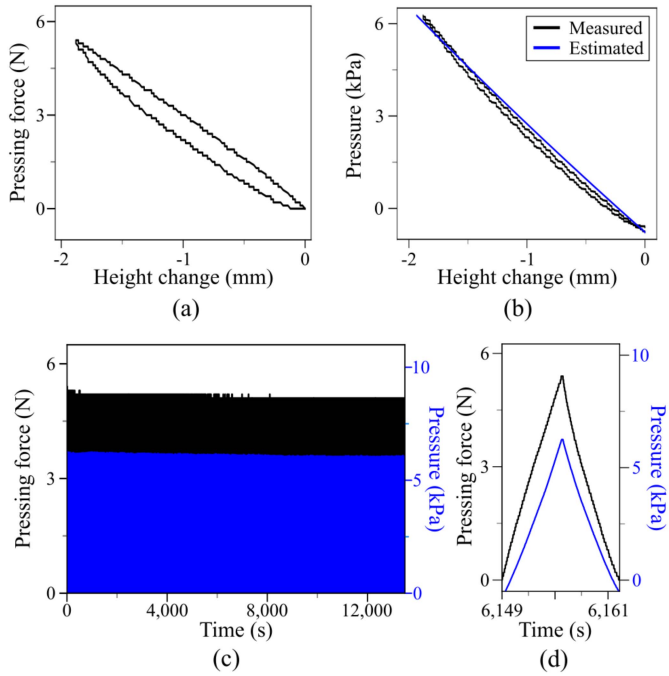

Fig. 13. Experimental results of barometric pressure sensor. (a) Measured force as the height of the gripper changes. (b) Measured pressure as the height of the gripper changes and comparison between height estimation (Blue) and actual measurement (Black). (c) Result of the cyclic test. (d) Force and sensor responses at 500th cycle.

force for the gripper is 50 N. In contrast, the gripper without compliance showed significant deformation of the fingertip when the pressing force of 20 N or higher was applied.

E. Characterization of Pressure Sensor

A barometric pressure sensor was connected to the air cover for contact detection and pressing force control. As discussed in Section II-D, we designed an experiment to determine the relationship between the pressing force and the height change of the gripper The sensor was characterized with its response to continuous force inputs. The repeatability of the sensor was also tested through a cyclic test.

The gripper was placed on the tensile tester (Mark-10) and pressed with a flat indenter by 2 mm. This travel distance generated a pressing force up to 5 N, which covered the range of the pressing force (3 N) for single sheet separation. The relationship between the pressing force and the change in height of the gripper is shown in Fig. 13(a), and the corresponding pressure measured by the sensor is shown in Fig. 13(b). The force measurement showed higher hysteresis during the loading and unloading process, than the pressure readings. We thus estimated Δh based on the measured pressure readings using the relationship presented in (5) and compared it to the experimental results [see Fig. 13(b)]. We confirmed that our model, based on Boyle's law, provided a reliable estimation of the actual pressure readings. Furthermore, the pressing force can be estimated with measurements from the pressure sensor using the result in Fig. 13(a).

The repeatability of the sensor was also tested over large cycles. From the initial state with no-load, the gripper tip was pressed down by 2 mm and released over 1000 cycles [see Fig. 13(c)]. During the cyclic test, the gripper demonstrated consistent changes in pressing force and internal pressure. This proves the structural robustness of the gripper and the fully sealed compliant posts during the test. Fig. 13(d) shows an sample of the force and the pressure profiles during the test.

IV. Application

We tested the proposed gripper with an application of picking up fabric sheets with automatic sensing and control. The gripper was mounted on the industrial robot arm (UR5e, Universal Robots), and the air source was connected to both the pinching and the suction chambers of the gripper through vacuum regulators (ITV2090, SMC). The 1–1 fabric was placed on a flat surface and the gripper pressed the fabric before picking it up. When the force estimated by the pressure sensor reached 0.5 N, it was recognized as a contact. Then, a vacuum pressure of −80 kPa was applied to the suction chamber to check the permeability of the target fabric. The actual vacuum pressure was measured by the vacuum regulator. All the air-permeable fabrics showed the pressures higher than −72 kPa, and the pressures for the non-air-permeable fabrics were between −80 to −72 kPa. A total of 90% of the applied vacuum pressure, was thus set as the threshold, used for autonomously determining the air permeability. In Fig. 14(a), the measured pressure was −67 kPa, indicating the air-permeable fabric was in contact. Then, the gripper pressed the fabric down with a force of 1.35 N based on the pressure sensor reading, which was the appropriate level of force required for single sheet separation for the 1–1 fabric [see Fig. 9(a)]. The pinching sequence can be found in Fig. 14(c). Next, a non-air-permeable fabric (2–1) was tested with the same process [see Fig. 14(b)]. In this case, a vacuum pressure of −77 kPa was used as the decision value for a non-air-permeable fabric. After identification of the permeability, suction was applied, and the gripper was able to lift the fabric. Since the gripping performance for the non-air-permeable fabrics was not affected by additional pressing force, the same force of 1.35 N was used for pinching. In this application, the gripper demonstrated successful gripping and separation of individual sheets without any human interventions or prior information on the height of the fabric.

We tested our gripper with a custom-designed soft manipulator made of bellow-type pneumatic actuators [see Fig. 15(a)]. To assist human operators in sophisticated fabric handling processes, a manipulator made of soft materials will be highly useful for safe interactions. We installed two grippers at the end of the soft manipulator to perform lifting and folding tasks of fabric sheets. The contact between the system and the fabric was first detected by a soft pressure sensor made of liquid-metal patterns embedded in an elastomer matrix [see Fig. 15(b)]. The grippers then picked up the fabric [see Fig. 15(c)] and moved it to the designated location [see Fig. 15(d)]. The gripper finally released and folded the fabric [see Fig. 15(e)].

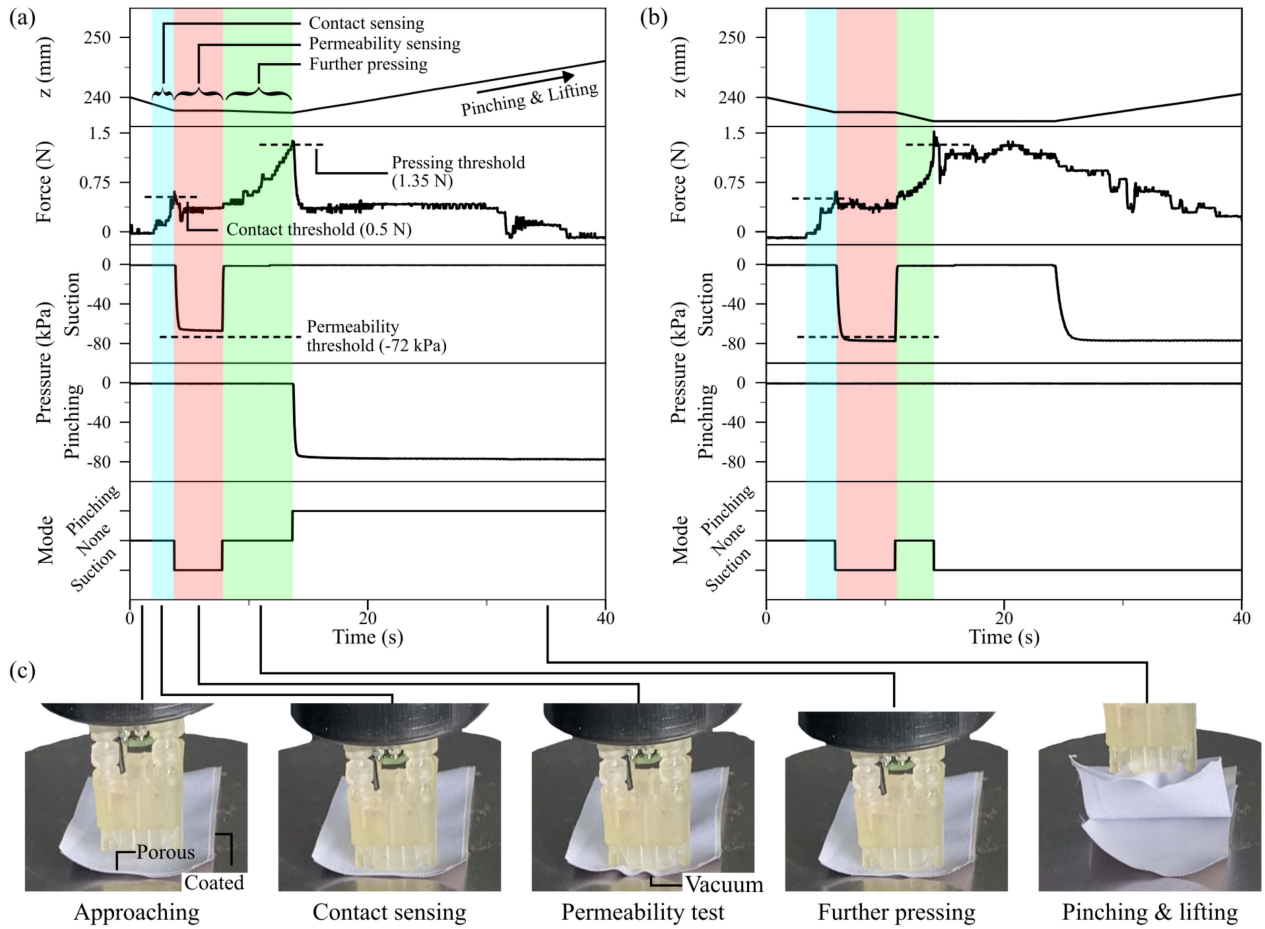

Fig. 14. Automatic fabric handling using proposed gripper system. (a) Sequence of picking up air-permeable fabric placed on coated non-air-permeable fabric. (b) Sequence of picking up coated non-air-permeable fabric. (c) Actual images of pinching sequence.

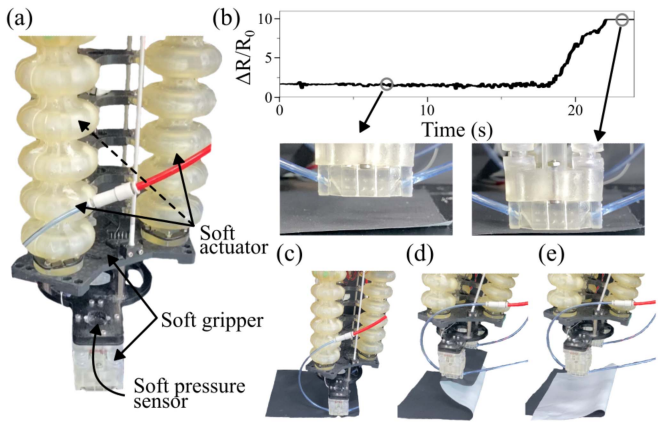

Fig. 15. Fabric handling soft manipulation system. (a) Custom-built soft manipulator equipped with the proposed grippers. (b) Soft pressure sensor reading up to contact with fabric. (c)–(e) Fabric handling process: fabric gripping, movement to the designated location, and releasing and folding the fabric, respectively.

V. Discussion

The main contribution of this study is development of a soft gripper made of a single structure that performs two actuation modes for delicate handling of a variety of fabrics. The gripper utilizes two different gripping mechanisms depending on the types of the target fabrics: pinching and suction for air-permeable and non-air-permeable fabrics, respectively. Bellow-shaped posts provide structural compliance for the gripper, allowing its easy conformation to the surface of the fabric for a stable contact. Even if the attack angle is not perfectly perpendicular to the surface of the fabric, the gripper makes a successful grip of the fabric, significantly simplifying the control algorithm and the installation process of the gripper. The integrated barometric pressure sensor detects the contact force, enabling autonomous operation as well as preventing an excessive load to the gripper In this way, the operation becomes fast and accurate, taking only two seconds to separate a sheet of fabric from a stack. In addition, since the gripper body is 3D-printed as a whole, the microneedles can be easily replaced using the needle holder, simplifying the manufacturing and the maintenance of the gripper in practical applications. Thus, our proposed gripper system demonstrates a high potential in automation of garment manufacturing processes.

In spite of the many advantages, there still exists rooms for improvements in design and function. For a more robust and autonomous fabric handling, an additional function can be added to cross-check the success of single sheet separations.

This may be achieved by adding capacitive sensors to the tip of the gripper [35], [36], [37] to measure the thickness of the fabric held between the fingertips. The performance of single sheet separation can also be enhanced by actively controlling the exposed length of the needles for a wide range of fabric thickness. Since thin fabrics require shallow penetration by the needles so that the needles engage only the top layer, we can dynamically control the protruded length of the needles depending on the thickness of the target fabric. This also allows more freedom to choose the pressing force within the range shown in Fig. 9(a). Active control of the length of the needle will also help easy separation of the needles from the fabric, not only extending the lifetime of the gripper but also reducing the possibility of damaging the fabric. To further improve the robustness and the repeatability, an air port could be added to the air cover and connected to the solenoid valve. Then, the pressure inside the air chamber could be adjusted to the ambient pressure after every actuation cycle. In addition, the resolution of the integrated pressure sensor could be further increased by using a more precise pressure sensor, enabling detection of small weight differences, i.e., the number of fabric sheets lifted.

The proposed gripper has unique design features for multimodal actuation, compliance, and sensing, which help handling of a variety of fabrics, single-sheet separation, and autonomous operation. Furthermore, our gripper can be fabricated with a high consistency by 3D printing.

VI. Conclusion

We developed a multifunctional soft gripper for handling various types of fabrics regardless of their air permeability. The proposed gripper is able to separate and pick up a single fabric sheet from a stack using two different gripping modes, pinching and suction, depending on the air permeability of the fabrics. The compliant structure of the gripper not only protects its fingertip from structural damages caused by excessive loads, but also ensures the gripping performance even in nonideal contact conditions. The integrated pressure sensor also allows detection of contact for automated control of the gripper. The gripper showed a robust and consistent performance over 10 000 cycles of repeated actuation. Therefore, we believe that the proposed gripper will play an important role in the field of future garment manufacturing where safety, convenience, and autonomous operation are critical.

References

[1] A. Tabiei and Y. Jiang, "Woven fabric composite material model with material nonlinearity for nonlinear finite element simulation," *Int. J., Solids Struct.*, vol. 36, no. 18, pp. 2757–2771, 1999.

[2] T. Ishikawa and T.-W. Chou, "Nonlinear behavior of woven fabric composites," *J. Compo. Mater.*, vol. 17, no. 5, pp. 399–413, 1983.

[3] P. Koustoumpardis and N. A. Aspragathos, "A review of gripping devices for fabric handling," in *Proc. Int. Conf. Intell. Manipulation Grasping*, 2004, pp. 229–234.

[4] Y. Duan, M. Keefe, T. Bogetti, and B. Cheeseman, "Modeling friction effects on the ballistic impact behavior of a single-ply high-strength fabric," *Int. J. Impact Eng.*, vol. 31, no. 8, pp. 996–1012, 2005.

[5] S. Terryn, J. Brancart, D. Lefeber, G. Van Assche, and B. Vanderborght, "Self-healing soft pneumatic robots," *Sci. Rob.*, vol. 2, no. 9, pp. 1–12, 2017.

[6] H. Zhao, K. O'Brien, S. Li, and R. F. Shepherd, "Optoelectronically innervated soft prosthetic hand via stretchable optical waveguides," *Sci. Rob.*, vol. 1, no. 1, 2016, Art. no. eaai 7529. .

[7] F. Ilievski, A. D. Mazzeo, R. F. Shepherd, X. Chen, and G. M. Whitesides, "Soft robotics for chemists," *Angew. Chem. Int. Ed.*, vol. 50, no. 8, pp. 1890–1895, 2011.

[8] Z. Xu and E. Todorov, "Design of a highly biomimetic anthropomorphic robotic hand towards artificial limb regeneration," in *Proc. IEEE Int. Conf. Rob. Autom.*, 2016, pp. 3485–3492.

[9] L. Jiang, K. Low, J. M. Costa, R. J. Black, and Y.-L. Park, "Fiber optically sensorized multi-fingered robotic hand," in *Proc. IEEE Int. Conf. Intell. Rob. Syst.*, 2015, pp. 1763–1768.

[10] S. J. Yoon, M. Choi, and Y.-L. Park, "Elongatable gripper fingers with integrated stretchable tactile sensors for underactuated grasping and dexterous manipulation," *IEEE Trans. Rob.*, vol. 38, no. 4, pp. 2179–2193, Aug. 2022.

[11] E. Brown et al., "Universal robotic gripper based on the jamming of granular material," *PNAS*, vol. 107, no. 44, pp. 18809–18814, 2010.

[12] Z. Zhakypov, F. Heremans, A. Billard, and J. Paik, "An origami-inspired reconfigurable suction gripper for picking objects with variable shape and size," *IEEE Rob. Autom. Lett.*, vol. 3, no. 4, pp. 2894–2901, Oct. 2018.

[13] Z. Xie et al., "Octopus arm-inspired tapered soft actuators with suckers for improved grasping," *Soft Rob.*, vol. 7, no. 5, pp. 639–648, 2020.

[14] Festo Corporation, "Vacuum suction cups," FESTO. Accessed: Jul. 2022. [Online]. Available: https://www.festo.com/us/en/c/products/industrial-automation/vacuum-technologies/vacuum-suction-cups-id_pim113/?

[15] T. T. Hoang, P. T. Phan, M. T. Thai, N. H. Lovell, and T. N. Do, "Bio-inspired conformable and helical soft fabric gripper with variable stiffness and touch sensing," *Adv. Mater. Technol.*, vol. 5, no. 12, 2020, Art. no. 2000724.

[16] S. Song, D.-M. Drotlef, D. Son, A. Koivikko, and M. Sitti, "Adaptive self-sealing suction-based soft robotic gripper," *Adv. Sci.*, vol. 8, no. 17, 2021, Art. no. 2100641.

[17] S. Ku, J. Myeong, H.-Y. Kim, and Y.-L. Park, "Delicate fabric handling using a soft robotic gripper with embedded microneedles," *IEEE Rob. Autom. Lett.*, vol. 5, no. 3, pp. 4852–4858, Jul. 2020.

[18] E. Ono, S. Nishikawa, H. Ichijo, and N. Aisaka, "New robot hand for cloth handling," *Sen'i Gakkaishi*, vol. 48, no. 9, pp. 501–506, 1992.

[19] P. I. Kaltsas, P. N. Koustoumpardis, and P. G. Nikolakopoulos, "A review of sensors used on fabric-handling robots," *Machines*, vol. 10, 2022, Art. no. 101.

[20] R. Sabeenian and M. Paramasivam, "Defect detection and identification in textile fabrics using multi resolution combined statistical and spatial frequency method," in *Proc. Int. Adv. Comput. Conf.*, 2010, pp. 162–166.

[21] P. Venkatraman, "Fabric properties and their characteristics," in *Material Technology Sportswear Performance Apparel*. Boca Raton, Florida: CRC Press, 2015, ch. 3, pp. 53–86.

[22] Y. Chen, D. Lloyd, and S. Harlock, "Mechanical characteristics of coated fabrics," *J. Text. Inst.*, vol. 86, no. 4, pp. 690–700, 1995.

[23] P. M. Taylor, D. Pollett, and M. Grieβer, "Pinching grippers for the secure handling of fabric panels," *Assem. Autom.*, vol. 16, no. 3, pp. 16–21, 1996.

[24] E. Ono, K. Kitagaki, and M. Kakikura, "On friction picking up a piece of fabric from layers," in *Proc. Int. Conf. Mechatron. Autom.*, 2005, pp. 2206–2211.

[25] E. Ono and K. Takase, "On better pushing for picking a piece of fabric from layers," in *Proc. Int. Conf. Rob. Biomimetics*, 2007, pp. 589–594.

[26] Y. Ebraheem, E. Drean, and D. C. Adolphe, "Universal gripper for fabrics–design, validation and integration," *Int. J. Clothing Sci. Technol.*, vol. 33, no. 4, pp. 643–663, 2020.

[27] Z. SachinT. Wang Matsuno, and S. Hirai, "Analytical modeling of a membrane-based pneumatic soft gripper," *IEEE Rob. Autom. Lett.*, vol. 7, no. 4, pp. 10359–10366, Oct. 2022.

[28] C. Tawk, A. Gillett, M. in het Panhuis, G. M. Spinks, and G. Alici, "A 3D-printed omni-purpose soft gripper," *IEEE Trans. Rob.*, vol. 35, no. 5, pp. 1268–1275, Oct. 2019.

[29] M. Zhu, Y. Mori, T. Wakayama, A. Wada, and S. Kawamura, "A fully multi-material three-dimensional printed soft gripper with variable stiffness for robust grasping," *Soft Rob.*, vol. 6, no. 4, pp. 507–519, 2019.

[30] D. Drotman, M. Ishida, S. Jadhav, and M. Tolley, "Application-driven design of soft, 3-D printed, pneumatic actuators with bellows," *IEEE/ASME Trans. Mechatron.*, vol. 24, no. 1, pp. 78–87, Feb. 2019.

[31] J. L. Matthews-Fairbanks, *Pattern Design: Fundamentals: Construction and Pattern Drafting for Fashion Design*. Fairbanks Publishing LLC, 2018.

[32] A. Jaiswal and B. Kumar, "Vacuum gripper-an important material handling tool," *Int. J. Sci. Technol.*, vol. 7, pp. 1–8, 2017.
[33] M. S. Xavier, A. J. Fleming, and Y. K. Yong, "Finite element modeling of soft fluidic actuators: Overview and recent developments," *Adv. Intell. Syst.*, vol. 3, no. 2, 2021, Art. no. 2000187.
[34] M. Wei, "The theory of the cantilever stiffness test," *J. Text. Inst.*, vol. 80, no. 1, pp. 98–106, 1989.
[35] P. Roberts, D. D. Damian, W. Shan, T. Lu, and C. Majidi, "Soft-matter capacitive sensor for measuring shear and pressure deformation," in *Proc. IEEE Int. Conf. Rob. Autom.*, 2013, pp. 3529–3534.
[36] C. B. Cooper et al., "Stretchable capacitive sensors of torsion, strain, and touch using double helix liquid metal fibers," *Adv. Funct. Mater.*, vol. 27, no. 20, 2017, Art. no. 1605630.
[37] O. Atalay, A. Atalay, J. Gafford, and C. Walsh, "A highly sensitive capacitive-based soft pressure sensor based on a conductive fabric and a microporous dielectric layer," *Adv. Mater. Technol.*, vol. 3, no. 1, 2018, Art. no. 1700237.

Subyeong Ku (Member, IEEE) received the B.S. degree from Yonsei University, Seoul, South Korea, in 2008, and the Ph.D. degree from Seoul National University, Seoul, South Korea, in 2023, both in mechanical engineering.

He is currently a Senior Researcher with Korea Automotive Technology Institute, Cheonan, South Korea. His research interests include, soft actuators, soft manipulator, machine learning, smart manufacturing, and process automation.

Byung-Hyun Song received the B.S. degree in mechanical engineering from Korea University, Seoul, South Korea, in 2022. Since then, he has been working toward the Ph.D. degree in mechanical engineering with Seoul National University, Seoul, South Korea.

His research interests include soft actuators and sensors, soft manipulator, and wearable robots.

Taejun Park received the B.S. degree in mechancial engineering from Seoul National University, Seoul, South Korea, in 2021. Since then, he has been working toward the Ph.D. degree in mechanical engineering with Seoul National University, Seoul, South Korea.

His research interests include, soft sensors, soft manipulator, and wearable systems.

Ho-Young Kim received the B.S. degree from Seoul National University, Seoul, South Korea, in 1994, and the M.S. and Ph.D. degrees from Massachusetts Institute of Technology, Cambridge, MA, USA, in 1996 and 1999, respectively, all in mechanical engineering.

He is currently a Professor of mechanical engineering with Seoul National University, Seoul, South Korea, and a Fellow of American Physical Society. His research activities revolve around microfluid mechanics, biomimetics, and soft matter physics.

Yong-Lae Park (Member, IEEE) received the M.S. and Ph.D. degrees in mechanical engineering from Stanford University, Stanford, CA, USA, in 2005 and 2010, respectively.

He is currently a Professor with the Department of Mechanical Engineering, Seoul National University (SNU), Seoul, South Korea. Prior to joining SNU, he was an Assistant Professor with the Robotics Institute, Carnegie Mellon University, Pittsburgh, PA, USA, from 2013 to 2017 and a Technology Development Fellow with the Wyss Institute for Biologically Inspired Engineering, Harvard University, Cambridge, MA, USA, from 2010 to 2013. His research interests include soft artificial skin sensors and muscle actuators, soft robotics, wearable robotics, biomedical and rehabilitation robotics, and novel manufacturing technologies for soft smart materials and structures.